

DFTT 6/1993
February 93

**COLLECTIVE MODES IN A SLAB
OF INTERACTING NUCLEAR MATTER:
The effects of finite range interactions**

W.M. Alberico

Dipartimento di Fisica Teorica dell'Università–Torino, Italy
and INFN, Sezione di Torino, Italy

P. Czerski

Institute of Nuclear Physics
ul. Radzikowskiego 152, Kraków, Poland

A. De Pace

Dipartimento di Fisica Teorica dell'Università–Torino, Italy
and INFN, Sezione di Torino, Italy
and

V.R. Manfredi

Dipartimento di Fisica dell'Università–Padova, Italy
and INFN, Sezione di Padova, Italy

ABSTRACT

We consider a slab of nuclear matter and investigate the collective excitations, which develop in the response function of the system. We introduce a finite-range realistic interaction among the nucleons, which reproduces the full G-matrix by a linear combination of gaussian potentials in the various spin-isospin channels. We then analyze the collective modes of the slab in the $S = T = 1$ channel: for moderate momenta hard and soft zero-sound modes are found, which exhaust most of the excitation strength. At variance with the results obtained with a zero range force, new “massive” excitations are found for the vector-isovector channel .

1. Introduction.

The slab of interacting nuclear matter has revealed itself as an interesting tool[1,2] for investigating specific properties of nuclei: being confined in one dimension only, it allows to consider, e.g., the influence of a surface (already present in the semi-infinite slab of Esbensen and Bertsch[3]) together with the effects of discrete levels, which are appropriate for a spatially confined system. But at the same time it keeps typical features of an infinite system, like for example density oscillations with phonon-like dispersion relation, together with translational invariance along the two unconfined directions.

This model also offers a schematic (and rather extreme) situation to be compared with the one of highly deformed nuclei: as already pointed out in ref.[2], the observed splitting of the dipole resonance can be related with the analogous phenomenon which shows up in the collective modes (zero sound) of the slab.

In this paper we consider, as in ref.[2], the response function of a slab of interacting nucleons within the framework of the Random Phase Approximation (RPA): however, while in the previous work a schematic zero range force (of the Landau–Migdal type) was employed, here we utilize a more realistic nucleon–nucleon interaction, which is derived by suitably fitting previous G–matrix calculations [4,5]. The effective interaction derived in the present work has the appropriate finite range in all spin–isospin channels and allows a more detailed investigation of the interplay between range of the interaction and size of the system. This point will be explored in connection with the collective modes of the slab, as derived within the RPA framework: indeed we will show how the corresponding response function is modified in the presence of finite range forces.

In Section 2 we briefly describe the model, summarizing the appropriate formalism to deal with the response function of the slab; in Section 3 we give the derivation of the effective particle–hole interaction, which is considered in the various spin–isospin channels. Finally in Section 4 the resulting RPA response function and, specifically, the collective modes of the slab are presented and shortly discussed.

2. Description of the model.

We consider, as in ref.[2], a system of noninteracting fermions, confined in the domain $0 \leq z \leq L$ by an infinite potential well; the single particle wave functions are then:

$$\langle \vec{r} | \vec{k} \rangle = \sqrt{\frac{2}{SL}} \exp \left[i \vec{k}_{\parallel} \cdot \vec{r}_{\parallel} \right] \sin(k_{\perp} z) \chi_s \xi_t , \quad (2.1)$$

where S is the area of the surfaces which set the boundaries of the system (the slab), χ_s and ξ_t are two-component spinors in the spin and isospin space and the symbols \parallel and \perp correspond to the parallel and perpendicular directions to the slab surfaces. In (2.1), since at the end we shall let $S \rightarrow \infty$, k_{\parallel} is assumed to be a continuum wave number whereas k_{\perp} is quantized according to

$$k_{\perp} = n \frac{\pi}{L} = n \frac{k_F}{M} , \quad (2.2)$$

with $n=1,2,3,\dots$, the total particle wave number being $k = \sqrt{k_{\parallel}^2 + k_{\perp}^2}$. Eq.(2.2) also relates M with the slab thickness L and to the Fermi momentum k_F : since M has to be an integer number, by fixing the slab thickness k_F turns out to be quantized (or viceversa, indeed for convenience we will assume a fixed value for $k_F = 1.36 \text{ fm}^{-1}$).

From the single particle wavefunctions and (kinetic energy) eigenvalues one can obtain the polarization propagator (or particle-hole Green function) for the non-interacting Fermi gas of nucleons in the slab; it reads

$$\Pi^0(x_1, x_2) = -\frac{4i}{\hbar} G^0(x_1, x_2) G^0(x_2, x_1) \quad (2.3)$$

where G^0 is the free single particle Green's function and the factor of 4 arises from the traces over spin and isospin (we assume an isospin symmetric, $N=Z$, nuclear matter). The Fourier transform for the slab system is then defined as follows:

$$\begin{aligned} f(\vec{k}_{\parallel}, k_{\perp}, k'_{\perp}) &= S \int d^2 r_{\parallel} \exp \left[-i \vec{k}_{\parallel} \cdot \vec{r}_{\parallel} \right] \\ &\times \int_0^L dz_1 \int_0^L dz_2 \tilde{f}(\vec{r}_{\parallel}, z_1, z_2) \cos(k_{\perp} z_1) \cos(k'_{\perp} z_2) \end{aligned} \quad (2.4)$$

$$\begin{aligned} \tilde{f}(\vec{r}_{\parallel}, z_1, z_2) &= \frac{1}{(2\pi)^2} \frac{4}{L^2} \frac{1}{S} \int d^2 k_{\parallel} \exp \left[i \vec{k}_{\parallel} \cdot \vec{r}_{\parallel} \right] \\ &\times \sum_{k_{\perp}, k'_{\perp}} f(\vec{k}_{\parallel}, k_{\perp}, k'_{\perp}) \cos(k_{\perp} z_1) \cos(k'_{\perp} z_2) \eta_{k_{\perp}} \eta_{k'_{\perp}} \end{aligned} \quad (2.5)$$

where \vec{k}_{\parallel} should be thought of as $\vec{k}_{\parallel} - \vec{k}'_{\parallel}$ since the system is translational invariant in the direction parallel to the surface and $\eta_{k_{\perp}} = 1(1/2)$ for $k_{\perp} \neq 0$ ($k_{\perp} = 0$). By applying the above transformations to the polarization propagator (for details and explicit formulas see ref.[2]) we calculate the real and imaginary part of $\Pi_{\text{slab}}^0(\vec{k}_{\parallel}, k_{\perp}, k'_{\perp}, \omega)$.

We remind that the imaginary part of the polarization propagator is directly related to the response function of the system, thus providing the excitation strength of the slab when this is coupled to an external probe; if the latter, for example, induces charge density fluctuations into the system, the response per particle is given by the relation:

$$R(k_{\parallel}, k_{\perp}, \omega) = -\frac{2}{N\pi} \text{Im} \Pi_{\text{slab}}^0(k_{\parallel}, k_{\perp}, k_{\perp}, \omega) . \quad (2.6)$$

As already stated in the introduction, in this work we are mainly concerned with the effects of a realistic interaction on the slab response function, and with the interplay between the finite range of the force and the finite size of the system. These items are best investigated within the framework of the Random Phase Approximation (RPA) scheme. We have already pointed out in ref.[2] the main differences between the infinite nuclear matter and the slab RPA equations for the polarization propagator. Due to the finite size of the slab in the transverse dimension, translational invariance is lost and the simple algebraic RPA equation[6] for the polarization propagator in nuclear matter turns into a set of coupled equations for the non-diagonal elements of $\Pi_{\text{slab}}^{\text{RPA}}$ in momentum space.

In order to derive the latter it is convenient to start with the RPA equation for the polarization propagator in r-space; it reads (the subscript “slab” is omitted to simplify the notation):

$$\begin{aligned} \Pi^{\text{RPA}}(\vec{r}_1 - \vec{r}_2, z_1, z_2) &= \Pi^0(\vec{r}_1 - \vec{r}_2, z_1, z_2) + \int d^2 r_3 d^2 r_4 \int_0^L dz_3 dz_4 \\ &\times \Pi^0(\vec{r}_1 - \vec{r}_3, z_1, z_3) V(\vec{r}_3 - \vec{r}_4, z_3, z_4) \Pi^{\text{RPA}}(\vec{r}_4 - \vec{r}_2, z_4, z_2) \end{aligned} \quad (2.7)$$

where the \vec{r}_i are two dimensional vectors in the (x,y)-plane. Since the interaction is time independent, we shall not explicitly indicate the time (or energy) dependence in our formulas.

Applying now the cosine Fourier transformation, defined in (2.4) and (2.5), to both sides of (2.7) we get, after some manipulations, the compact expression

$$\sum_{k''_\perp} \left[\delta_{k_\perp, k''_\perp} - \frac{4}{L} \rho_{\text{slab}} \sum_{k''_\perp} \eta_{k''_\perp} \eta_{k''_\perp} \Pi^0(k_\parallel, k_\perp, k''_\perp) V(k_\parallel, k''_\perp, k''_\perp) \right] \Pi^{\text{RPA}}(k_\parallel, k''_\perp, k'_\perp) = \Pi^0(k_\parallel, k_\perp, k'_\perp) . \quad (2.8)$$

This equation is easy to solve numerically since the transverse momenta are discretized according to $k_\perp = nk_F/M$ ($n = 0, 1, 2 \dots$) and the longitudinal momentum k_\parallel can take arbitrary values and plays the role of a fixed parameter. For a definite choice of k_\parallel and ω (which is implicit in the free and RPA polarization propagators), eq. 2.8 becomes a two-dimensional system of linear algebraic equations. We cut the range of the allowed k_\perp -values when it exceeds by more than three times the upper limit of the corresponding response region for the free system. Moving to k_\perp values higher than k_\perp^{\max} does not affect the results by more than one percent and doesn't change the qualitative features of the solution.

Concerning the particle-hole interaction $V(k_\parallel, k'_\perp, k''_\perp)$ between nucleons in the slab system, it is derived from a finite range realistic NN potential, as it will be explained in the next Section. We anticipate here that in nuclear matter it is represented by a linear combination of gaussian functions both in momentum space,

$$V(k) = g e^{-k^2/m^2}, \quad (2.9)$$

where g and m are fitting parameters, and in r-space, where it reads, correspondingly,

$$V(r) = C e^{-\mu r^2}, \quad (2.10)$$

with $\mu = m^2/4$, $C = g(m^3/8\pi^2)\sqrt{\pi}$.

For the slab system we have to perform the Fourier cosine transformation (2.4) on gaussian functions like (2.10) and the resulting particle-hole force (apart from the spin-isospin matrix elements) turns out to be of the following form:

$$V(k_\parallel, k'_\perp, k''_\perp) = SC \frac{\pi}{\mu} e^{k_\parallel^2/4\mu} \int_0^L \int_0^L dz_1 dz_2 e^{-\mu(z_1 - z_2)^2} \cos(k'_\perp z_1) \cos(k''_\perp z_2), \quad (2.11)$$

where the integration over z_1, z_2 has to be carried out numerically. As a result of the finite range of the interaction $V(k_\parallel, k'_\perp, k''_\perp)$ is neither diagonal with respect to k'_\perp and k''_\perp nor constant in momentum space (at variance with ref.[2]).

3. The Effective Interaction.

To proceed with the calculation of the RPA response function, we need the finite range potential which acts between nucleons. We start from any realistic NN potential derived by fitting the NN scattering data and, in order to properly deal with the strong short range correlations, we insert this “bare” interaction in the Bethe–Goldstone equation. In the operator form the latter reads:

$$G = V + V \frac{Q}{E - H_0} G \quad (3.1)$$

where V is the bare NN potential, G is the so called Brueckner G –matrix (which will coincide with our effective interaction), E is the starting energy, H_0 is the Hamiltonian operator for the intermediate two–particle states; finally Q is the Pauli operator, which takes care of the medium effects of the Fermi system, by forbidding the particles to scatter into occupied intermediate states.

The Bethe–Goldstone equation is then solved in the infinite nuclear matter, following the method suggested by Haftel and Tabakin[7]. Eq.(3.1) implicitly depends upon the density of the system via the Pauli operator; we fix the starting energy to be $E=74$ MeV. Further details can be found in references [4,5]. As a solution we have the so called G –matrix, which can then be expressed in terms of the direct and exchange matrix elements of an effective potential: the latter is subsequently represented by means of a suitable parameterization.

The method we employ has been developed in ref.[5]: working in the particle–hole representation, one interprets the resulting G –matrix as direct plus exchange matrix elements of some effective potential, whose dependence upon spin and isospin operators is explicitly taken into account. Then the momentum dependence of this potential is suitably parameterized in terms of simple Yukawa’s functions, with the aim of obtaining an effective potential which is vaguely related to the exchange of some “effective” mesons.

For the purpose of applications to the slab system the Yukawa’s form of the interaction hinders the (partially) analytical evaluation of the particle–hole force (2.11). Thus in the present work we have considered a local parameterization of the G –matrix elements in the form of simple gaussians. These might turn quite advantageous also for finite nuclei calculations, e.g. when the single particle wave functions are expressed in terms of Harmonic Oscillator eigenstates.

To illustrate the fitting procedure let us consider the particle–hole matrix elements of G in a definite spin–isospin channel, $\langle ST|G(\vec{k}, \vec{p}_1, \vec{p}_2)|ST\rangle \equiv \langle ST|U_{ph}|ST\rangle$; as

shown in Fig.1, the direct matrix element depends on the total p–h momentum \vec{k} while the exchange one depends upon $\vec{p}_1 - \vec{p}_2$ (the center of mass dependence being taken into account by some averaging procedure).

We now assume that the momentum dependence of the G–matrix, solution of eq.(3.1) with some realistic input for the NN bare potential, can be accurately reproduced by a two–body potential of the form:

$$U_{ph}(\vec{q}) = g_{00} e^{-q^2/m_{00}^2} \mathbb{1}_\sigma \mathbb{1}_\tau + g_{01} e^{-q^2/m_{01}^2} \mathbb{1}_\sigma (\vec{\tau}_1 \cdot \vec{\tau}_2) + g_{10} e^{-q^2/m_{10}^2} (\vec{\sigma}_1 \cdot \vec{\sigma}_2) \mathbb{1}_\tau + g_{11} e^{-q^2/m_{11}^2} (\vec{\sigma}_1 \cdot \vec{\sigma}_2) (\vec{\tau}_1 \cdot \vec{\tau}_2), \quad (3.2)$$

where for sake of simplicity we do not include tensor components, which could be extracted as well by considering definite spin projections in the G–matrix elements. Considering, for example, the $S = 0, T = 0$ channel, the p–h matrix element of (3.2) reads (with the same notation of Fig.1):

$$\begin{aligned} <00|U_{ph}|00> &= g_{00} \left(4e^{-k^2/m_{00}^2} - e^{-(\vec{p}_1 - \vec{p}_2)^2/m_{00}^2} \right) \\ &- 3g_{01} e^{-(\vec{p}_1 - \vec{p}_2)^2/m_{01}^2} - 3g_{10} e^{-(\vec{p}_1 - \vec{p}_2)^2/m_{10}^2} - 9g_{11} e^{-(\vec{p}_1 - \vec{p}_2)^2/m_{11}^2}. \end{aligned} \quad (3.3)$$

With the approximation $\vec{p}_1 - \vec{p}_2 \simeq 0$ (which turns out to be accurate, at least for not too large particle momenta) the exchange contributions simply reduce to a constant and, in order to fix the parameters in the effective potential U_{ph} , eq.(3.2), one has to solve the following system:

$$\begin{aligned} <00|G(k)|00> &= g_{00} \left(4e^{-k^2/m_{00}^2} - 1 \right) - 3g_{01} - 3g_{10} - 9g_{11} \\ <01|G(k)|01> &= -g_{00} + g_{01} \left(4e^{-k^2/m_{01}^2} + 1 \right) - 3g_{10} + 3g_{11} \\ <10|G(k)|10> &= -g_{00} - 3g_{01} + g_{10} \left(4e^{-k^2/m_{10}^2} + 1 \right) + 3g_{11} \\ <11|G(k)|11> &= -g_{00} - g_{01} + g_{10} + g_{11} \left(4e^{-k^2/m_{11}^2} - 1 \right) \end{aligned} \quad (3.4)$$

This allows to extract strengths (g_{ST}) and masses (m_{ST}) for all components in U_{ph} . In order to obtain a good fit to the original solution two gaussians are needed for each spin–isospin channel. Moreover we found it more convenient (and accurate) to find separate parameterization for the full G-matrix elements and for the direct part of them. For example, in the $S = T = 0$ channel one sets:

$$<00|G|00>_{\text{tot}} = 4 \left(g_{00,F}^{(1)} \exp\{-k^2/(m_{00,F}^{(1)})^2\} + g_{00,F}^{(2)} \exp\{-k^2/(m_{00,F}^{(2)})^2\} \right), \quad (3.5a)$$

$$\langle 00|G|00 \rangle_{\text{dir}} = 4 \left(g_{00,D}^{(1)} \exp\{-k^2/(m_{00,D}^{(1)})^2\} g_{00,D}^{(2)} \exp\{-k^2/(m_{00,D}^{(2)})^2\} \right). \quad (3.5b)$$

The parameters of the present fit are summarized in Table I for the direct part of the G-matrix and in Table II for the full interaction. We observe that, at variance with ref.[5], the present parameterization involves the full G-matrix and not only the corrections induced by the ladder diagrams on the original bare potential (which in some cases are artificially large); thus one does not need the explicit knowledge of the NN interaction employed in the Bethe–Goldstone equation. The effective particle–hole potential resulting from our fit is illustrated in Fig.2, where the full p–h interaction is displayed for each spin–isospin channel and compared with the exact G-matrix. The quality of the fit is fairly good, but for the scalar isoscalar channel, which however will not be utilized in the following: indeed in this case the interaction turns out to be strongly attractive over the whole range of momenta and cannot produce the hard collective modes we are interested in.

4. Results and discussion.

We have solved the RPA equations (2.8) for the slab polarization propagator by utilizing the effective potential of the previous Section. As one can see from Fig.2 the full interaction develops a large repulsive p–h force in the spin–isospin channel ($S = T = 1$), together with a rather strong momentum dependence; the latter (although we are neglecting the tensor components of the interaction) should be ascribed to the presence, in this channel, of the long range one pion exchange potential. As it is well known[8] the attractive pion exchange modulates the strong repulsive short range correlations in the spin–isospin channel, thus producing some softening of the RPA response function.

From the resulting momentum dependence of the p–h force we expect indeed to observe a different behaviour, in the collective response of the system, with respect to ref.[2], where a zero–range (constant in momentum space) interaction was used within the same theoretical framework. One should also remind that the interaction utilized here is not diagonal in the perpendicular momentum, thus involving a larger influence of the non–diagonal terms of Π in the RPA equations (2.8).

Let us then focus on the vector–isovector channel: it is well known that, in nuclear matter, at small energy and momentum transfers the repulsive interaction is strong enough to produce a collective excitation (zero sound) outside the continuum p–h response, which in turn is severely depressed.

In the slab system and with the present finite range interaction we have found, in analogy with ref.[2], two distinct collective modes, according whether the transfer momentum is parallel to the infinite dimensions of the system or perpendicular to it: in Fig.3a,b we display these zero sound dispersion relations, which have approximately a linear form: $\omega = vk$, v being the corresponding velocity of propagation of the bosonic excitation in the nuclear medium. Results are displayed for infinite nuclear matter and for slabs with two different thicknesses (which are fixed by the value of the integer M). Fig.3b shows a magnified view of Fig.3a at somewhat larger momentum transfers, where one can better distinguish the different modes occurring for the $M = 2$ and $M = 8$ slabs.

More precisely, the sound velocity in nuclear matter turns out to be $v_s^{n.m.} = 1.62v_F$ (it would be $v_s^{n.m.} = 1.71v_F$ with a δ -force of approximately the same strength as the one of the gaussian interaction at $q = 0$); $v_F = 0.286c$ is the Fermi velocity. For the $M = 2$ slab the two sound velocities obtained with our gaussian interaction are (in parenthesis the corresponding values for the δ -force) $v_{\parallel} = 1.36v_F$ ($1.5v_F$) and $v_{\perp} = 1.54v_F$ ($1.89v_F$), for the parallel and perpendicular modes, respectively. In a thicker slab ($M = 8$) the resulting sound velocities are closer to each other and to the infinite nuclear matter value: $v_{\parallel} = 1.56v_F$ ($1.67v_F$) and $v_{\perp} = 1.58v_F$ ($1.79v_F$).

With respect to the analogous outcome in ref.[2] one should notice the following qualitative differences :

- i) the dispersion relation in nuclear matter is modified by the present interaction, since as the momentum increases the p-h force weakens (see Fig.2) thus producing some softening with respect to a constant interaction;
- ii) for a fixed thickness of the slab, one still finds two distinct collective modes, the faster of which being associated with a transverse momentum transfer (“perpendicular” mode), however *both* the perpendicular and the parallel modes lie *below* the nuclear matter curve, while in the previous work they were sitting on opposite sides. This outcome should signal the role played by the off-diagonal (in the perpendicular momentum) terms of the interaction, which were absent for the δ -force and produce a sizeable softening both of the longitudinal and, even more, of the transverse modes.
- iii) we remark that the above discussed softening is due to the attractive part of the interaction and this, in turn, has to be associated with pion exchange, namely with the longest range component of the NN force. It is thus worth noticing that the relative lowering of the transverse zero sound velocity is much larger than the one of the parallel mode: this fact signals an important correlation between the

range of the interaction and the transverse dimension of the slab, where the finite size of the system plays the major role.

Beside the previously illustrated collective modes, the present model displays additional excitations, which in the RPA scheme are signalled by poles in $\text{Re}\Pi^{RPA}$, not occurring in Π^0 , corresponding to very narrow peaks in $\text{Im}\Pi^{RPA}$ (and thus in the response function); this is shown in Fig.4, for the $M = 8$ slab. The energy–momentum dispersion relation of these modes, which occur at higher energies with respect to the zero sound, differs from the latter since it does not vanish in the zero momentum limit and then stays almost constant, with a weak quadratic dependence. They are illustrated in Fig.5, for the $M = 2$ and $M = 8$ slabs: in the thicker system the energy interval between any two of these modes is smaller (they appear to be almost equally spaced); however the strength in the corresponding peaks (see Fig.4) rapidly goes down. Indeed they disappear in the infinite system.

The origin of these collective excitations lies in the finite range of the interaction utilized here and critically depends upon the interplay between range of the interaction and extension of the system: they did not show up when a zero–range force was employed, as in ref.[2]. Moreover the peaks seem to be more pronounced when the range of the interaction (2–3 fm) is comparable with the transverse dimension of the slab: in the $M = 8$ slab ($L \simeq 18$ fm) only the lowest energy mode displays a significant strength.

This situation resembles the low frequency modes occurring in crystals and in spin systems (ferromagnets, antiferromagnets, etc.): in both cases one observes (one or more) acoustical and optical branches, the former having vanishing frequency when $k \rightarrow 0$, the latter requiring finite excitation energy in the long wavelength limit. In a ferromagnetic system the above mentioned excitations are spin waves usually called magnons[9]: experimental evidence for these modes has been revealed by inelastic neutron scattering[10]. From the microscopic point of view, they could be explained in terms of collective excitations of an infinite range Ising model[11], which allows to associate the finite frequency of the optical branch to the order parameter of the ferromagnetic phase.

In the present case we notice that the above mentioned “massive” modes have been found in the spin–isospin channel ($S = T = 1$) and may be explored by letting the system to interact with an external electromagnetic field. They arise only when the interaction has a *non-zero range* and disappear when translational invariance is restored, by letting $L \rightarrow \infty$; indeed in infinite nuclear matter the zero sound alone is allowed as a collective mode, irrespective on the (finite or zero) range of the model

interaction utilized. It is worth reminding that the only physical example of a similar mode occurring in an infinite system, the electron gas, are the so-called plasmons, whose origin is driven by the infinite range of the Coulomb potential. Here instead we have finite range forces and the “plasmon–like” excitations survive only as far as the range of the interaction is comparable with the slab thickness L . Actually in the infinite system the three different types of collective excitations which we have found (parallel and perpendicular zero sound, and plasmon–like) collapse into a single collective mode, with linear dispersion relation.

It might be interesting to notice that in a Wigner lattice the occurrence of a similar situation has been interpreted in connection with the phenomenon of spontaneous symmetry breaking. This model displays three different types of elementary excitations: two transverse modes which behave as phonons, with $\omega \propto q$, and a longitudinal collective mode (the “plasmon”) which has a finite frequency as $q \rightarrow 0$ [12–14]. According to Anderson the plasmon can be viewed as the massive “Higgs” boson associated with the spontaneous breaking of gauge invariance which is due, in the presence of the Coulomb potential, to the density fluctuations in the electron gas. Notably, the existence of this massive mode is crucially related to the long range of the Coulomb interaction. Short range correlations, like in crystals, would give rise to massless Goldstone bosons alone.

As a final remark we would like to point out that the present calculation, although rather crude in the description of the nuclear confinement, yet utilizes a realistic p–h force, thus allowing to bear some confidence in the qualitative (if not quantitative) results we obtain for the collective excitations of the system. In particular we believe that the analysis of the interplay between the range of the interaction and the finite size of the system might offer some hints also for experimental research in highly deformed nuclei.

Acknowledgements

The authors wish to thank Prof. A. Molinari for fruitful discussions.

Work was partially supported by Grant No. KBN 202049101.

REFERENCES.

- [1] W. M. Alberico, A. Molinari and V. R. Manfredi, Phys.Lett. **B194**, 1-5 (1987);
- [2] W.M. Alberico, P. Czerski, V.R. Manfredi and A. Molinari, Zeit. für Physik **A338**, 149-155 (1991);
- [3] H. Esbensen and G. F. Bertsch, Annals of Physics **157**, 255-281 (1984);
- [4] W.H. Dickhoff, Nucl. Phys. **A399** (1983) 287;
- [5] P. Czerski, W.H. Dickhoff, A. Faessler, and H. Müther, Nucl. Phys. **A427** (1984) 224;
- [6] see, for example, A. L. Fetter and J. D. Walecka, *Quantum Theory of Many-Particle systems* (McGraw-Hill, New York, 1971);
- [7] M.I. Haftel and F. Tabakin, Nucl. Phys. **A158** (1970), 1;
- [8] W.M.Alberico, M.Ericson and A.Molinari, Phys. Lett. **92B** (1980), 153;
- [9] C.Kittel, *Quantum theory of solids*, John Wiley and Sons (1987);
- [10] Brockhouse and Watanabe, IAEA Symposium, Chalk River, Ontario, 1962;
- [11] J.W. Negele and H.Orland, *Quantum Many-Particle Systems*, Addison-Wesley Pub. Co. (1988);
- [12] P.W.Anderson, Phys. Rev. **130** (1963), 439
- [13] P.W.Anderson, *Basic Notions of Condensed Matter Physics* Frontiers in Physics, (1984) Benjamin/Cummings Publ. Co.
- [14] E.Wigner and F.Seitz, Phys. Rev. **43** (1933), 804; **46** (1934), 509.

Table I

Direct Matrix Element				
S T	$g_{ST}^{(1)}$ [MeV fm ³]	$m_{ST}^{(1)}$ [MeV]	$g_{ST}^{(2)}$ [MeV fm ³]	$m_{ST}^{(2)}$ [MeV]
0 0	-1014.40	4379.0	423.25	313.6
0 1	187.45	449.7	425.23	2773.5
1 0	-426.00	4478.2	163.00	654.8
1 1	-266.24	9553.0	272.70	370.8

Table I – Parameterization of the Direct p–h matrix elements of the G–matrix of ref.[4,5]; S, T denote the total spin and isospin quantum numbers of the relevant channels.

Table II

Direct+Exchange Matrix Element				
S T	$g_{ST}^{(1)}$ [MeV fm ³]	$m_{ST}^{(1)}$ [MeV]	$g_{ST}^{(2)}$ [MeV fm ³]	$m_{ST}^{(2)}$ [MeV]
0 0	-2865.64	862.0	185.90	862.0
0 1	576.20	10000.0	576.2	377.0
1 0	321.14	9691.0	606.16	669.8
1 1	1307.6	461.0	-388.74	1363.0

Table II – Parameterization of the Direct+Exchange p–h matrix elements of the G–matrix of ref.[4,5]; notations are the same as in Table I.

Figure Captions

Fig. 1 – Graphical representation of the direct (a) and exchange (b) particle–hole matrix element of the interaction.

Fig. 2 – The present gaussian fit (continuous lines) to the p–h matrix elements of the full (direct plus exchange) G–matrix (dashed lines) is presented as a function of k (in fm^{-1}) for the various spin–isospin channels. The units on the vertical scales are MeV fm^3 .

Fig. 3 – The zero sound dispersion relations for the infinite nuclear matter (continuous line) and for two slabs with $M = 2$ and $M = 8$: the parallel modes correspond to the short–dashed ($M = 2$) and dotted ($M = 8$) lines, while the transverse modes (which are not visible in upper part (a) of the figure) are represented by the dashed and dot–dashed curves, respectively. The latter must be considered as interpolations, to guide the eye, of the discrete– q points where the transverse zero sound can be found.

Fig. 4 – $\text{Re}\Pi^{\text{RPA}}$ (dotted line) and $\text{Im}\Pi^{\text{RPA}}$ (continuous line) for the $M = 8$ slab, at $q_{\parallel} = 0.4 \text{ fm}^{-1}$, $q_{\perp} = 0$, versus energy.

Fig. 5 – Energy versus momentum behaviour of the collective modes in the parallel direction for the $M = 2$ slab (dashed lines) and the $M = 8$ slab (dotted lines); the infinite nuclear matter zero sound is also displayed (continuous line).

Fig. 1

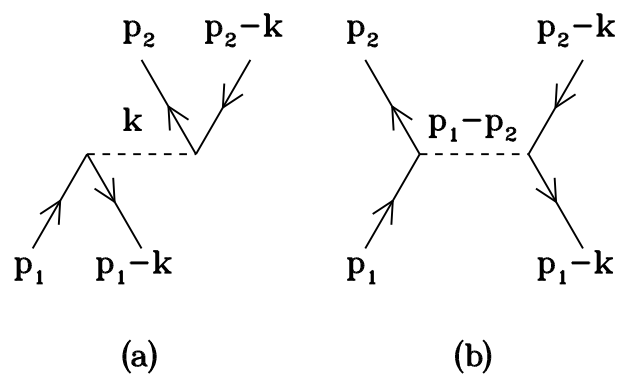


Fig.2

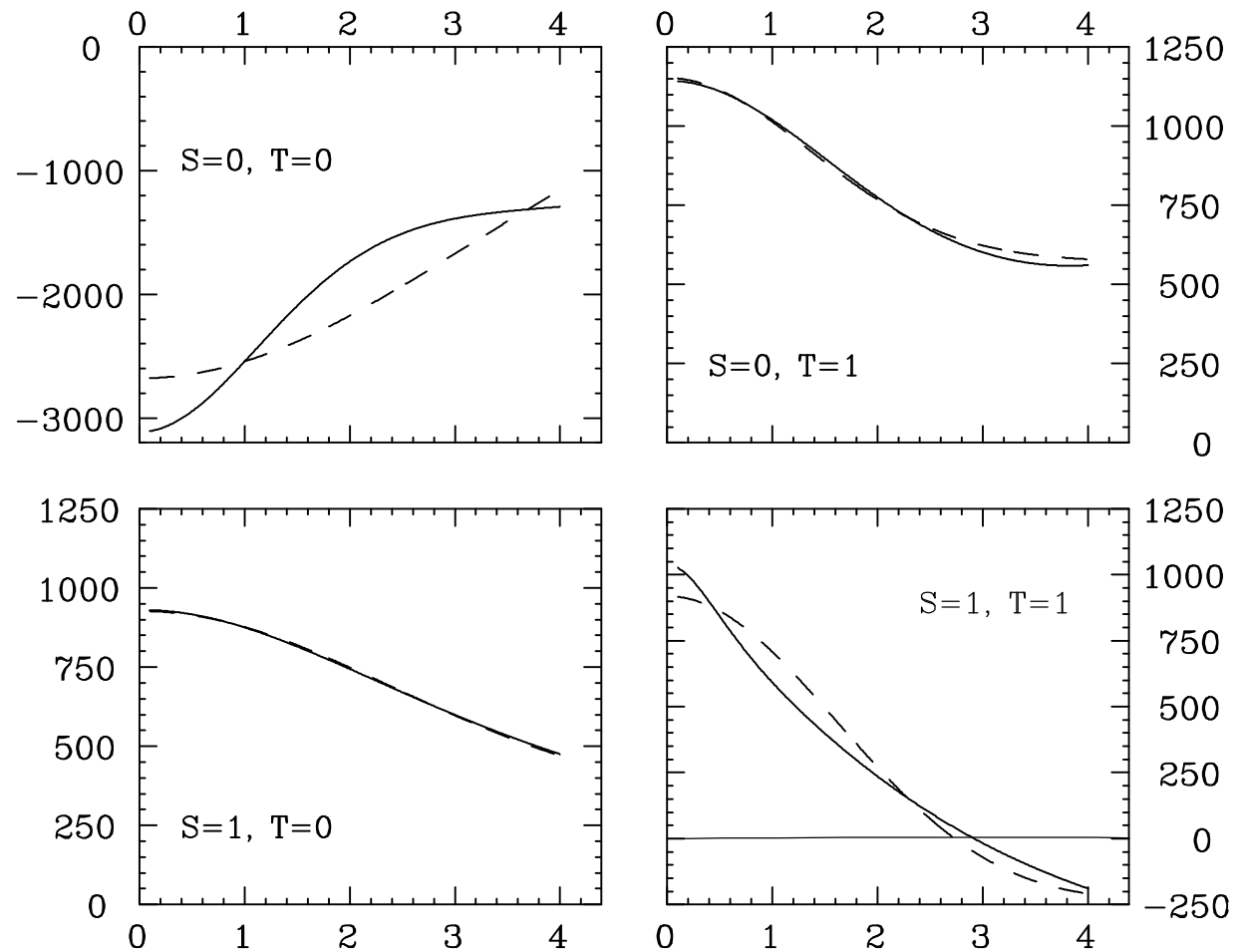


Fig.3

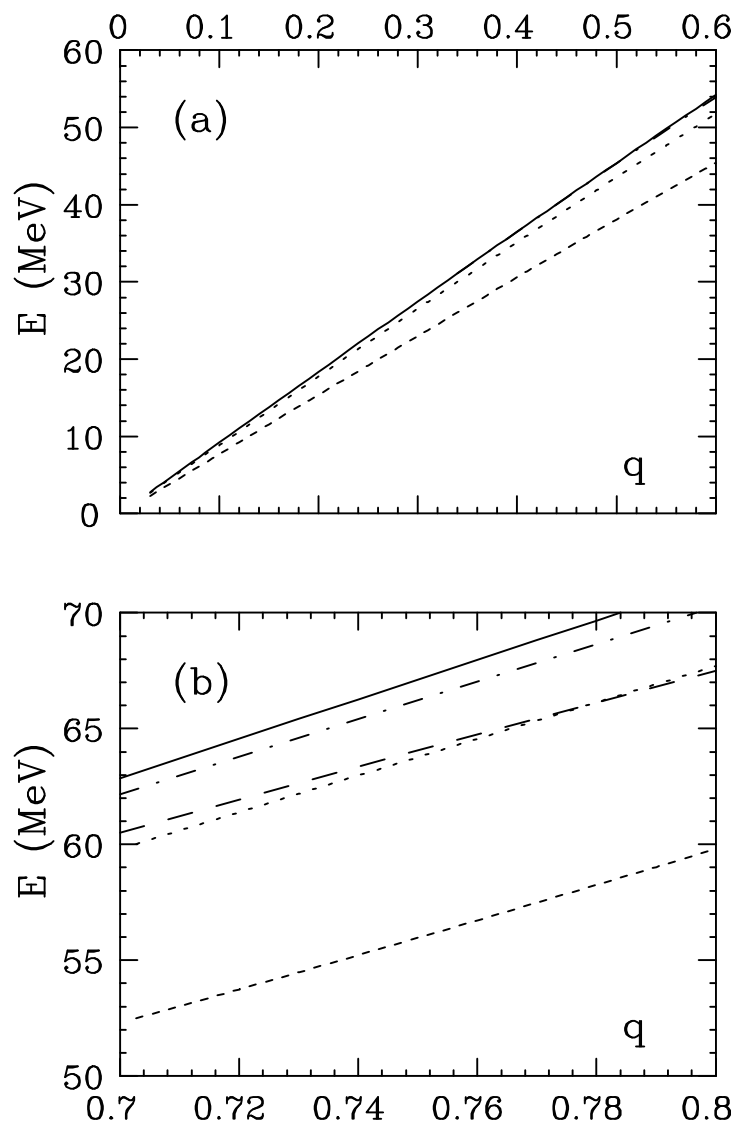


Fig.4

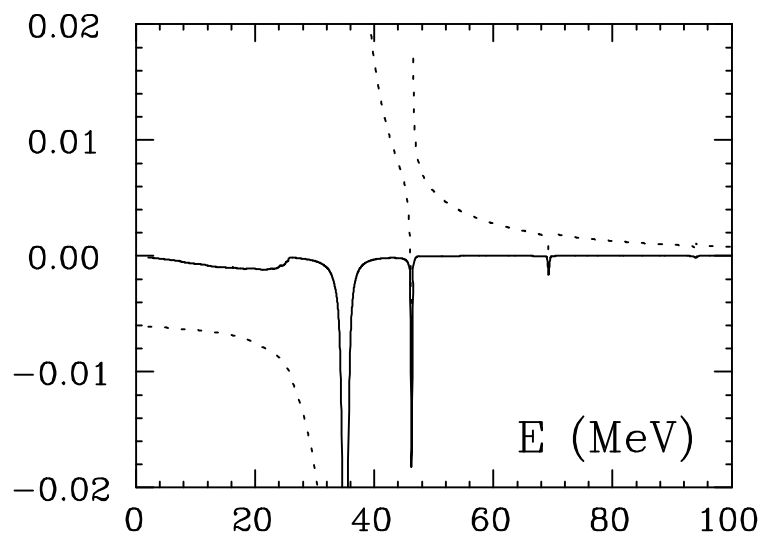


Fig.5

